

# **The Denaturation of Cytochrome *c* and Cytochrome *c* as Peroxidase**

by

**Lei Wang**

B.S. Wuhan University, 2003

Submitted to the Graduate Faculty of  
Arts and Sciences in partial fulfillment  
of the requirements for the degree of  
Master of Science

University of Pittsburgh

2006

UNIVERSITY OF PITTSBURGH

School of Arts and Sciences

This thesis was presented

by

Lei Wang

It was defended on

Jan 26<sup>th</sup>, 2006

and approved by

David H. Waldeck, Professor, Department of Chemistry

Adrian C. Michael, Associate Professor, Department of Chemistry

Sunil K. Saxena, Assistant Professor, Department of Chemistry

Thesis Director: David H. Waldeck, Professor, Department of Chemistry

Copyright © by Lei Wang

2006

# **The Denaturation of Cytochrome *c* and Cytochrome *c* as Peroxidase**

Lei Wang, M.S.

University of Pittsburgh, 2006

Conformational transitions of proteins play a crucial role in many biochemical and biophysical reactions. Understanding the conformational changes of a protein upon adsorption to a substrate is very important in biotechnology, e.g. the development of modern protein chip technology, biocompatibility of implants, and many other ones. This research program used cytochrome *c*, an electron carrier in the respiratory chain, as a model to probe how surface adsorption affects the folding of a protein. My work investigates the interaction of protein horse heart cytochrome *c* when it is electrostatically adsorbed or covalently attached onto a 1 nm thick monolayer film, which covers an Au surface. After changing the pH value of the solutions or adding the denaturants into the solutions, the conformation of cytochrome *c* changes and causes a change of the peak current of cyclic voltammogram. In addition, the denatured cytochrome *c*'s peroxidase activity will be studied and compared with the peroxidase activity of microperoxidase-11.

## TABLE OF CONTENTS

<b>PREFACE</b> .....	<b>VIII</b>
<b>1.0 INTRODUCTION</b> .....	<b>1</b>
<b>2.0 BACKGROUND</b> .....	<b>4</b>
<b>2.1 CYTOCHROME C AND ITS EARLY STUDIES</b> .....	<b>4</b>
<b>2.2 ELECTRON TRANSFER IN RESPIRATORY CHAIN</b> .....	<b>6</b>
<b>2.3 APOPTOSIS</b> .....	<b>9</b>
<b>3.0 EXPERIMENTAL SECTION</b> .....	<b>11</b>
<b>3.1 CHEMICALS</b> .....	<b>11</b>
<b>3.2 ELECTRODE PREPARATION</b> .....	<b>11</b>
<b>4.0 RESULTS AND DISCUSSION</b> .....	<b>14</b>
<b>4.1 DENATURATION OF CYTOCHROME C</b> .....	<b>14</b>
<b>4.2 CYTOCHROME C AS PEROXIDASE</b> .....	<b>23</b>
<b>4.3 OXYGEN REACTION</b> .....	<b>31</b>
<b>5.0 CONCLUSION</b> .....	<b>34</b>
<b>6.0 FUTURE PLANS</b> .....	<b>37</b>
<b>APPENDIX A</b> .....	<b>39</b>
<b>BIBLIOGRAPHY</b> .....	<b>41</b>

## LIST OF FIGURES

<i>Figure 1. Multiprotein complexes in the respiratory assembly</i> .....	7
<i>Figure 2. standard reduction potentials of the major respiratory electron carriers.</i> .....	8
<i>Figure 3. Cyclic voltammograms of covalently attached Cyt c on mixed carboxylic SAM ( 40% 16-MHDA and 60% 14-MTOH) at different scan rate in 10 mM phosphate buffer, pH 7. The inset shows the cyclic voltammograms at the scan rate of 25 mV/s.</i> .....	15
<i>Figure 4. Fitting of experimental peak separation as a function of scan rate to Butler-Volmer model. The data are from Figure 3.</i> .....	17
<i>Figure 5. cyclic voltammograms of covalently attached Cyt C on mixed carboxylic SAM ( 40% 16-MHDA and 60% 14-MTOH) at different pH. Scan rate: 500 mV/s.</i> .....	18
<i>Figure 6. Variation of the peak currents during the acid titration. The ■ points represent anodic peak currents, and the ○ points represent the shift of the Soret bands of cyt c in free solution obtained by Cheng<sup>4</sup></i> .....	19
<i>Figure 7. Variation of the peak currents by increasing the urea concentration in pH 7 phosphate buffer. The cyclic voltammograms of covalently attached Cyt C on mixed carboxylic SAM ( 40% 16-MHDA and 60% 14-MTOH ) were recorded at the scan rate: 500 mV/s. The ■ points represent anodic peak currents, and the ○ points represent the fractional populations of native protein in solution obtained by Russell.<sup>1</sup></i> .....	20
<i>Figure 8. time dependent cyclic voltammograms of CL/cyt c complex immobilized onto mixed carboxylic SAM. Solution condition: 2 mM TOCL/ 2 mM PC liposome in 10 mM pH 7.0 phosphate buffer. Scan rate: 30 V/s</i> .....	22
<i>Figure 9. Cyclic voltammograms of different concentration H<sub>2</sub>O<sub>2</sub> in pH 3, 1M phosphate buffer, at a gold electrode modified by cytochrome c. Scan rate: 500 mV/s</i> .....	23

*Figure 10. Cyclic voltammograms of different concentration  $H_2O_2$  in pH 3, 1 M phosphate buffer, at a gold electrode coated with mixed carboxylic SAM. Scan rate: 500 mV/s..... 26*

*Figure 11. Charge dependence on concentration of  $H_2O_2$ . ..... 28*

*Figure 12. Cyclic voltammograms of different concentration  $H_2O_2$  in pH 7, 10 mM phosphate buffer, at a gold electrode modified by liposome denatured cytochrome c. Scan rate: 30 V/s .... 29*

*Figure 13. Cyclic voltammograms of gold electrode modified by denatured cytochrome c in 10 mM pH 3 phosphate buffer with or without  $O_2$ . Scan rate: 1 V/s ..... 31*

## PREFACE

First of all, I would like to thank Dr. Waldeck for his very helpful guidance and generous support. His precise research attitude, broad knowledge not limited to chemistry, but all other sciences, especially physics and mathematics, inspires me to explore and get close to the truth behind the phenomenon.

I also want to thank my collaborator Liana Basova, Igor Kurnikov and Dr. Kagan, through whom I can view my research from another perspective. I learned a lot of things from them.

Hongjun taught me the basic experiment steps when I just joined this group. His patience helped me get used to the new research quickly.

For the rest of the group members, Min, Pallu, Subhasis, Amit and Li, I feel proud to work with them. On the way to challenge the unknowns, I work in a team but not by myself.

Finally, I want to thank cordially my parents for their persistent care and encouragement, no matter where I am, how I am and what I am. I have been missing them so much!

## 1.0 INTRODUCTION

Conformational transitions of proteins play a crucial role in many biochemical and biophysical reactions. Understanding the conformational changes of a protein upon adsorption to a substrate is very important in biotechnology, e.g. the development of modern protein chip technology, biocompatibility of implants, and other phenomena.<sup>2,3</sup> In many applications, it is important that a protein retains its activity when it binds onto the substrate. To achieve this goal, the substrate is usually modified by a self-assembled monolayer (SAM)<sup>5</sup> to which proteins can be adsorbed electrostatically or attached covalently. This research program used cytochrome *c*, which is an electron carrier in the respiratory chain, as a model to probe how surface adsorption affects the folding of a protein.

A number of workers have studied the folding and unfolding of cytochrome *c*<sup>6,7</sup> and it has been reported that cytochrome *c* can be denatured by urea<sup>8,9</sup>, guanidine hydrochloride<sup>10,11</sup> or pH<sup>4,12-14</sup>. A great deal of valuable information on specific aspects of cytochrome *c* folding has been obtained from a variety of spectroscopic techniques.<sup>15</sup> For example, nuclear magnetic resonance (NMR) has probed the solvent exposure of exchangeable protons on the polypeptide backbone.<sup>16</sup> Techniques such as circular dichroism (CD)<sup>17</sup> and small-angle X-ray scattering<sup>18</sup> provide information on the secondary structure content and average molecular size of the protein molecule, respectively. Tryptophan fluorescence and optical absorption spectroscopies provide information about local interchain interactions by taking advantage of the presence of the heme

prosthetic group.<sup>19,20</sup> Resonance Raman spectroscopy has been demonstrated to be especially useful in visualizing folding intermediates along the folding coordinate.<sup>21,22</sup>

Cytochrome *c* plays a key role during apoptosis. Apoptosis describes a common type of programmed cell death that has been repeatedly observed in various tissues and cell types. After releasing to the cytosol, cytochrome *c* binds Apaf-1 (apoptotic protease-activating factor-1) and activates procaspase 9 to form a complex designated apoptosome. Activated caspase-9 can activate other caspases that ultimately destroy the cell.<sup>23</sup> Through apoptosis, a multicellular organism can tightly control cell numbers and tissue size, and protect itself from rogue cells that destroy homeostasis.

Cytochrome *c* is positively charged at neutral pH and the inner mitochondrial membrane contains a large fraction of negatively charged phospholipids, cardiolipin.<sup>24</sup> Cytochrome *c* interacts electrostatically with the inner membrane in the mitochondria. It has been shown that once bound to cardiolipin, cytochrome *c* will change its conformation and chemical reactivity.<sup>25</sup> Cytochrome *c* plays a critical role in early apoptosis as a cardiolipin-specific oxygenase to produce cardiolipin hydroperoxides required for the release of proapoptotic factors. Hence, the peroxidase activity of cytochrome *c* is very important. When cytochrome *c* is in its native state, the heme pocket is wrapped by the peptide chain and protected by the solvent, even though it is located near the protein edge. When cytochrome *c* is unfolded by lowering the pH or increasing the concentration of denaturants, the heme pocket loses its integrity, and can unwrap to expose the heme to solvent molecules. Easy access of the heme pocket can facilitate the hydroperoxide catalyzing reaction.

In the research below, the denaturation of cytochrome *c* and its peroxidase activity are characterized by cyclic voltammetry. Cyclic voltammetry allows one to monitor the redox

reaction as cytochrome *c* is unfolded. For the denatured cytochrome *c*, adding H<sub>2</sub>O<sub>2</sub> into the buffer solution causes a great enhancement of current, and the current is stable even after several continuous scans. Moreover, the current increased with the concentration of H<sub>2</sub>O<sub>2</sub> and the cytochrome *c*'s peroxidase activity was enhanced by binding to cardiolipin.

In the current study, we considered the interplay between the peroxidase activity and the conformation of cytochrome *c* with the ultimate goal to better understand the specificity of mitochondrial lipid oxidation in apoptosis.

## 2.0 BACKGROUND

### 2.1 CYTOCHROME C AND ITS EARLY STUDIES

In the early 1920s, David Keilin observed a typical four-banded cytochrome spectrum of flight muscles of the adult fly, *Gastrophilus*, whose larval form spends most of its life hanging on the inside of the stomach of the horse and carries a considerable amount of a hemoglobin-like pigment. The same spectrum was found in a large variety of species including both animals and plants, and the observed components were termed “cytochrome”.<sup>6</sup> Cytochrome *c* is an electron carrier in the respiratory chain and has become an extremely popular protein.<sup>26,27</sup> It plays an important role in a wide range of fields of biochemistry, molecular biology and cell biology.

Cytochrome *c* has been well investigated by structural studies,<sup>28-31</sup> spectroscopic properties,<sup>32,33</sup> thermodynamic properties,<sup>34-36</sup> electron transfer kinetics<sup>37</sup> and mutant studies<sup>38</sup> for many decades. The first x-ray structural study of cytochrome *c* was obtained for the horse heart cytochrome *c* in 1962. The molecule has a shape of a prolate spheroid with axial dimensions of 25×25×37 Å. The most important details of its structure were already known in the mid-1970s and include 1) the heme is covalently attached to the protein through two thioester bonds to cysteines 14 and 17. 2) the “closed crevice” in which the heme iron is held, with the axial ligands histidine 18 and the methionine 80. 3) the presence of five  $\alpha$ -helical segments, notably the N-terminal (residues 2-14), the C-terminal (residues 87-103), and the helical segments 49-55, 60-

70, and 70-75. These the structural properties dictate the function of cytochrome *c*. At present, five kinds of cytochrome *c* structures are known at sufficiently high resolution to allow for detailed studies: yeast iso-1, yeast iso-2, tuna, horse and rice. Moreover, these structures have proven central to the process of understanding the mechanism of cytochrome *c* mediated electron transfer events.

One of the most fundamental of all properties of a protein is the ability to fold spontaneously to a unique three-dimensional structure. The goal of studies of protein folding is to understand the physical mechanisms by which amino acid sequence determines protein structure and stability. Cytochrome *c* has played an important role in understanding these mechanisms.<sup>6,7</sup>

Since the biological function of cytochrome *c* is to carry out oxidation-reduction reactions, it follows that measurements of the oxidation-reduction potentials and associated electron transfer kinetics are central to its understanding. The formal redox potential for the ferri/ferrocyanochrome *c* couple is 0.265 V versus NHE (pH 7),<sup>34</sup> and is known to vary with temperature,<sup>35</sup> pressure,<sup>36</sup> electrolyte composition and ionic strength.<sup>39</sup> It is well known that cytochrome *c* can be strongly adsorbed on Pt, Hg, Au, Ag and other electrodes. The adsorption has been shown to result in conformational changes of the cytochrome *c*, protein unfolding and often its denaturation. To solve this problem, chemically modified electrodes, in particular with self-assembled monolayers(SAM), have been widely used to inhibit the denaturation while maintaining electroactivity. Cytochrome *c* has a net positive charge. When SAMs composed of carboxylic acid-terminated thiols present a negatively charged surface, cytochrome *c* binds electrostatically to the surface. The assembly provides a direct model to study the electron transfer reaction. If the methylene chain length is larger than 6, the nonadiabatic electron transfer

rate constant  $k^0$  of cytochrome  $c$  appears to depend exponentially on distance. The decay coefficient  $\beta$  is close to 1.1 per methylene group when the number of methylene groups  $n$  in the chain is larger than 8. Interestingly, when  $n$  is smaller than 6,  $k^0$  depends weakly on distance, showing a 'plateau region'. This phenomenon suggests two different mechanisms of electron transfer for the thin and thick SAM films.<sup>40</sup>

## 2.2 ELECTRON TRANSFER IN RESPIRATORY CHAIN

As human-beings, we convert chemical energy into bioactivity everyday and compensate the loss of chemical fuel by consuming food. Microscopically, energy is stored in the form of ATP within the cell, and it is released by converting ATP into ADP. ATP is synthesized from ADP in mitochondria.



A mitochondrion consists of four distinct subregions, the outer membrane, the inner membrane, the intermembrane space and the matrix. Whatever the compartment in which biological oxidation occurs, all of these processes generate reduced electron carriers, primarily NADH. When this NADH is reoxidized by the enzymes of the respiratory chain which are firmly embedded in the inner membrane, ATP is regenerated.<sup>41</sup>

The inner membrane is highly folded into cristae throughout the interior of the mitochondrion. Because the protein carriers, primarily cytochromes, which constitute the respiratory chain, are embedded within the inner membrane, the density of cristae is related to the respiratory activity of a cell. The higher the rate of respiration within a cell, the more densely the packed cristae within a mitochondrion. For example, horse heart cells, which have a high rate

of respiration, contain mitochondria with densely packed cristae. By contrast, liver cells, which have a slow rate of respiration, contain mitochondria with sparsely distributed cristae.

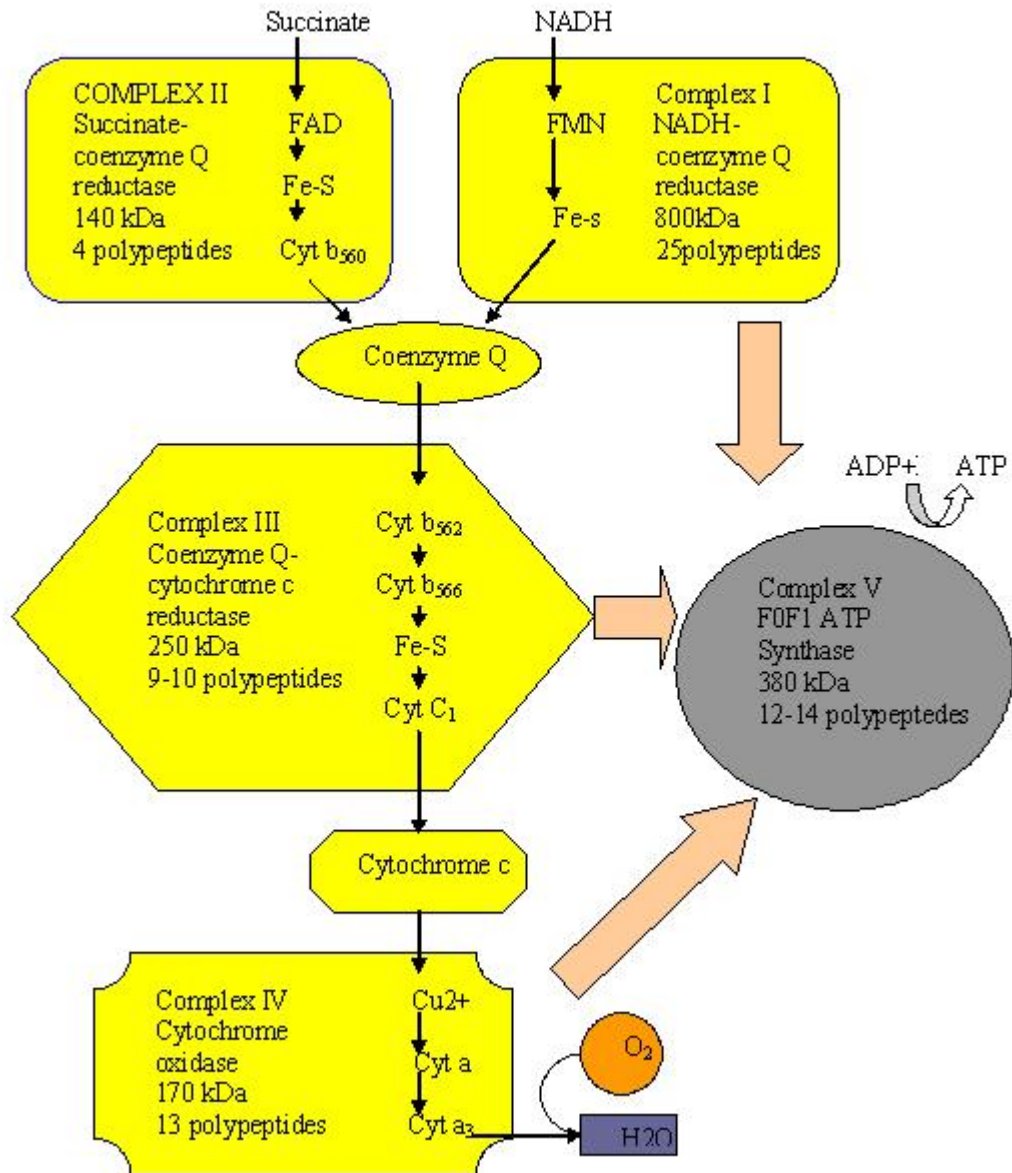


*Figure 1. Multiprotein complexes in the respiratory assembly*

The protein carriers in the respiratory chain are assembled in the form of five multiprotein complexes, named complex I, II, III, IV and V (Fig 1). Complex I and complex II receive

electrons from the oxidation of NADH and succinate, respectively, and pass them along to a lipid electron carrier, coenzyme Q, which moves freely through the membrane. Complex III gets the electron from coenzyme Q and passes it to cytochrome *c*. Finally, complex IV oxidizes the reduced form of cytochrome *c* and in turn reduces oxygen into water. The electron transfer process creates a proton gradient across the inner membrane, with protons being collected in the intermembrane space. Protons reenter the inner membrane through a specific channel in complex V. This process provides the necessary energy to drive the synthesis of ATP from ADP and inorganic phosphate.<sup>41</sup>

If you compare the sequence of respiratory electron carriers with the standard reduction potentials of those carriers (Fig 2), you will see that  $E'_0$  for each carrier increases in the same order as the sequence of their use in electron transport. This order suggests that each individual redox reaction in electron transport is exergonic under standard conditions.

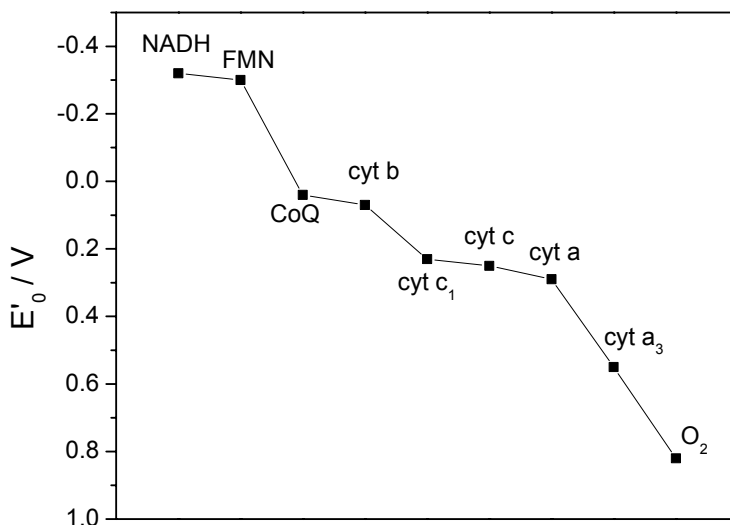


Figure 2. standard reduction potentials of the major respiratory electron carriers.

## 2.3 APOPTOSIS

Apoptosis, coined by Currie and colleagues in 1972, describes a common type of programmed cell death that has been repeatedly observed in various tissues and cell types.<sup>42</sup> This kind of programmed cell death is distinct from pathological cell death or necrotic cell death. Cells undergoing apoptosis show characteristic morphological features such as condensation of cytoplasmic and nuclear contents, blebbing of plasma membranes, fragmentation of nuclei, and ultimately breakdown into membrane-bound apoptotic bodies that are rapidly phagocytosed.<sup>23</sup> The stimuli, like cells in excess, or potentially dangerous cells, will often trigger the release of proapoptotic proteins into the cytosol, then activation of caspases and a proteolytic cascade occurs, which finally results in apoptosis. In this way, a multicellular organism can tightly control cell numbers and tissue size, and protect itself from rogue cells that destroy homeostasis.<sup>43</sup>

The apoptotic regulators, the Bcl-2 family,<sup>44</sup> are a key factor for determining the fate of a cell: life or death. This Bcl-2 family consists of over a dozen proteins, which can be divided into three groups, based on structural similarities and functional criteria. Group I, such as Bcl-2 and Bcl-x<sub>L</sub>, has the feature that all its members possess anti-apoptotic activity and protect cells from death. Group II, such as Bax and Bak, shares this feature with pro-apoptotic activity. Group III, such as Bid and Bik, has the common feature which is the presence of ~12-16 amino acid BH3 domain.

Though the precise mechanism of how proapoptotic Bcl-2 members regulate the exit of cytochrome *c* is still unclear, two major models have been proposed.<sup>23</sup> The first model suggests Bcl-2 members insert into the lipid bilayer of the mitochondrial outer membranes and form channels that facilitate exit of cytochrome *c* and other apoptotic protein. This model is based on

crystallography that suggests the three-dimensional structure of Bcl-x<sub>L</sub> shares a similarity with the pore-forming domains of certain bacterial toxins, including diphtheria toxin (DT). Both structures contain two central hydrophobic helices surrounded by amphipathic  $\alpha$  helices. The suggested function of the pore-forming domain of DT is to allow the subunit of the toxin to transit from the interior of lysosomes into the cytosol. Like these bacterial toxins, several members of the Bcl-2 family, including Bax and tBid, insert into lipid vesicles and planar lipid membranes, destabilize phospholipids bilayer, oligomerize and form channels. So far, only indirect support for this model exists; for instance, adding Bax, Bak and Bid to isolated mitochondria derived from liver or Hela cells results in permeabilization of the outer mitochondrial membrane, but the structure of the mitochondria is preserved. The second model suggests that Bcl-2 members interact with other proteins resulting in rupture of the outer membrane, while the inner membrane conserved because of its larger surface area with its cristae.

Once released in the cytosol, cytochrome *c* binds Apaf-1 (apoptotic protease-activating factor-1) and activates procaspase 9 in the presence of dATP or ATP to form a complex designated apoptosome.<sup>45</sup> Activated caspase-9 can activate other caspases that ultimately destroy the cells. Fractionation of Hela cytosol revealed that three protein factors, Apaf-1, Apaf-2 and Apaf-3, are necessary and sufficient to cause cell death. Apaf-2 has been identified as cytochrome *c* and Apaf-3 has been identified as caspase-9 while Apaf-1 has been identified as the human protein, homologous to the *C. elegans* cell death protein CED-4.<sup>46</sup>

## 3.0 EXPERIMENTAL SECTION

### 3.1 CHEMICALS

All reagents were used as received. All aqueous solutions were prepared with 18.3 M $\Omega$  cm<sup>-1</sup> deionized water (Nanopure, Barnstead, Dubuque, IA).

Phosphate buffer solution was made by mixing 10mM potassium phosphate diabase (GR) aqueous solution and 10 mM potassium phosphate monobase monohydrate (GR) aqueous solution and 10mM phosphoric acid to the desired pH value. All the buffer solutions were stored below 5 °C to prevent bacteria from growing, and then they sat at ambient temperature for 1hr before use.

Electrodes used in all experiments were gold ball electrodes made from gold wire (0.5 mm diameter,99.99%, Alfa Aesar).

### 3.2 ELECTRODE PREPARATION

**Gold ball electrodes.** A gold wire (0.5 mm diameter,99.99%) was cleaned by reflux in concentrated nitric acid (68-70%) at 130 °C overnight and then was washed with deionized water. The tip of the gold wire was heated to form a ball of ~0.06-0.15 cm<sup>2</sup> surface area. The gold ball was reheated in the flame until glowing and then quenched in deionized water. This

annealing process was performed more than 15 times to make a smooth gold ball. The exposed Au wire was sealed in a glass capillary tube, and the Au ball tip was annealed and cooled in a high-purity stream of Ar gas.

**SAM solutions.** For the pure carboxylic acid-terminated SAMs, the concentration of the solution is 2 mM in absolute ethanol. For the mixed carboxylic acid-terminated and hydroxyl-terminated SAMs, the total concentration of the solution is 2 mM with the ratio of 1:1.

**Immobilization of cytochrome *c*.** Chemically modified electrodes were prepared by placing the gold ball electrodes into the SAM solution for overnight. After that, the electrodes were taken out from the solution, first rinsed with absolute ethanol, then rinsed with the supporting buffer solution (10 mM phosphate buffer pH 7), and finally dried by a stream of dry argon gas. To covalently immobilize cytochrome *c*, the modified electrodes were first placed into the 5 mM CMC (1-cyclohexyl-3-(2-morpholinoethyl) carbodiimide metho-p-toluenesulfonate) solution in 100 mM phosphate buffer pH 7 for half an hour to activate the carboxyl group in the SAM. After the activation, the electrodes were rinsed with supporting buffer solution again and placed into 100  $\mu$ M cytochrome *c* solution in 10 mM phosphate buffer pH 7 for 1 hour. To electrostatically immobilize cytochrome *c*, we just skip the carboxyl group activation step and directly put the modified electrodes into the cytochrome *c* solution. After rinsing by buffer, these electrodes were immediately used in voltammetry studies.

**Electrochemical Measurements.** A computer-controlled CHI 618B electrochemical workstation (CH Instruments, Austin, TX) equipped with faraday cage was used for all electrochemical measurements. The three-electrode cell was composed of a platinum counter electrode, a Ag/AgCl (1 M NaCl) reference electrode, and the SAM-coated Au as a working

electrode. The voltammetry measurements were performed in 10 mM phosphate buffer solution with different pH value under an argon atmosphere.

## 4.0 RESULTS AND DISCUSSION

### 4.1 DENATURATION OF CYTOCHROME C

Fig. 3 shows the cyclic voltammograms of native cytochrome *c* covalently attached onto a mixed C<sub>15</sub>COOH and C<sub>14</sub>OH SAM at pH 7.5. For an electroactive reactant adsorbed at a surface, and displaying Nernstian behavior, the *i*-*E* curve must satisfy the following equation:<sup>47</sup>

$$i = \frac{n^2 F^2 \nu A \Gamma^* (b_O / b_R) \exp[(nF / RT)(E - E^{0'})]}{RT \{1 + (b_O / b_R) \exp[(nF / RT)(E - E^{0'})]\}^2}$$

where *n* is number of electrons transferred, *F* is Faraday's constant,  $\nu$  is the voltage scan rate, *A* is the electrode active area,  $\Gamma^*$  is surface concentration of reactant, *b<sub>O</sub>* and *b<sub>R</sub>* are equilibrium parameters in an adsorption isotherm for the oxidized form (O) and the reduced form of reactant respectively (R), and *E*<sup>0'</sup> is the formal potential. The peak current is given by  $i_p = \frac{n^2 F^2}{4RT} \nu A \Gamma^*$ ,

and the peak potential by  $E_p = E^{0'} - \left(\frac{RT}{nF}\right) \ln\left(\frac{b_O}{b_R}\right)$ . For an ideal Nernstian reaction under

Langmuir isotherm conditions: (a) no interactions between the adsorbed species on the electrode surface, (b) no heterogeneity of the surface, (c) at high bulk activities, saturation coverage of the electrode by adsorbate of amount  $\Gamma_s$ ,  $E_{pa} = E_{pc}$ , and the full width at half-height (FWHH) of

either the cathodic or anodic wave is given by  $\Delta E_{p,1/2} = 3.53 \frac{RT}{nF} = \frac{90.6}{n} mV (25^\circ C)$

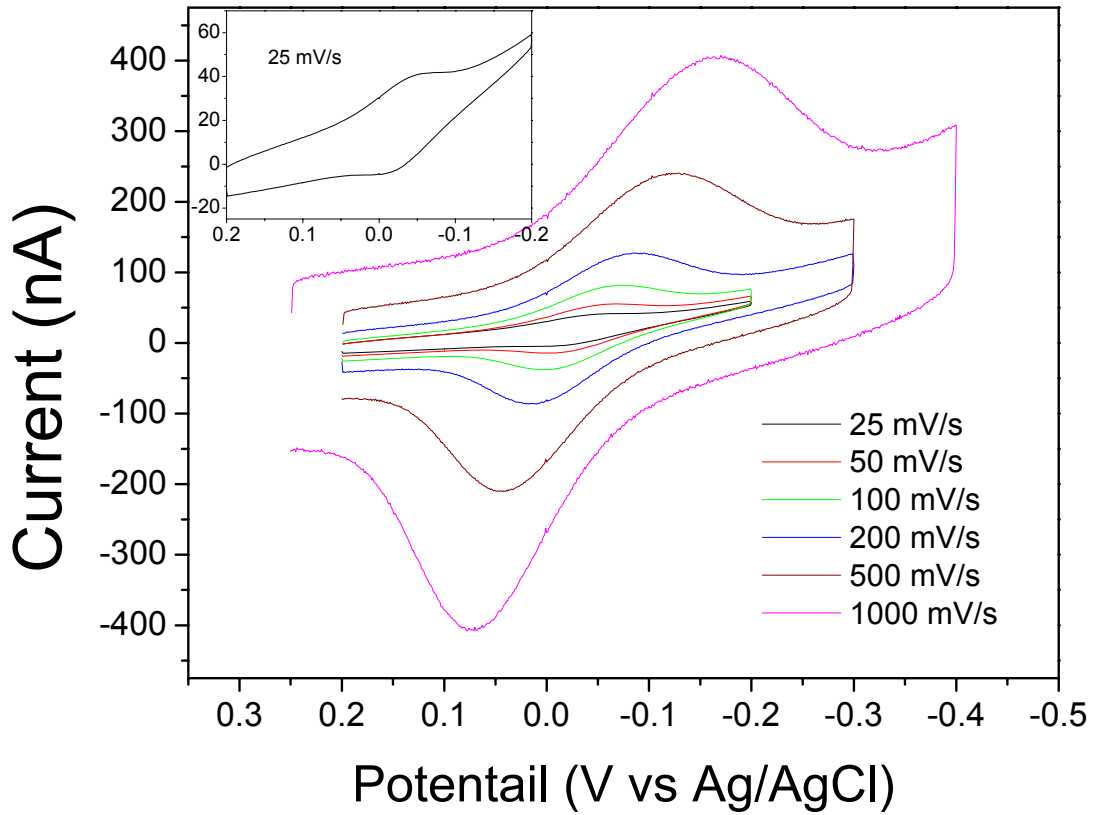


Figure 3. Cyclic voltammograms of covalently attached Cyt *c* on mixed carboxylic SAM ( 40% 16-MHDA and 60% 14-MTOH) at different scan rate in 10 mM phosphate buffer, pH 7. The inset shows the cyclic voltammograms at the scan rate of 25 mV/s.

For cytochrome *c* immobilized onto a SAM, at low scan rate (25 mV/s), the voltammogram after background subtraction is symmetric, the peak-peak separation is less than 10 mV, and the FWHHs for cathodic and anodic peaks are 92.3 mV and 91.5 mV respectively. Thus, the redox reaction at low scan can be approximated as reversible.

For a redox couple that is immobilized on the electrode surface, the peak current is given

by  $i_p = \frac{n^2 F^2}{4RT} \nu A \Gamma^*$ . For a mixed carboxylic SAM system, the observed current peak gives a

surface coverage of  $1.5 \pm 0.2 \times 10^{-12}$  mol/cm<sup>2</sup>, when cytochrome *c* is in its native state at pH =

7.5 and using  $n=1$ . This result is comparable to the data reported by Cheng et al.<sup>12</sup> The formal potential is found to be  $-0.032 \pm 0.008$  V with respect to Ag/AgCl/KCl (1M), that is  $0.203 \pm 0.008$  V with respect to NHE (pH 7). The formal potential of cytochrome *c* in solution was reported as 0.265 with respect to NHE (pH 7).<sup>34</sup> That is to say, the formal potential shifts negatively by about 60 mV when cytochrome *c* is absorbed into the surface. Because the formal potential is mainly determined by the heme, factors that will affect the heme structure will change the formal potential. The optical absorption spectra of cytochrome *c* in free solution and on the hydrophilic surface are pretty much the same, so that we assume the structure is similar.

The negative potential shift may be caused by the relative strength of adsorption of ferricytochrome *c* and ferrocyanochrome *c*. After cytochrome *c* is covalently attached to the SAM, cytochrome *c* still can interact electrostatically with adjacent carboxyl groups of the SAM. If the difference between electrostatic interact strength of ferricytochrome *c* and ferrocyanochrome *c* produces the negative formal potential shift, then we can use equation

$$E_p = E^{0'} - \left( \frac{RT}{nF} \right) \ln \left( \frac{b_o}{b_r} \right), \quad E^{0'} - E_p = 0.059V, \text{ to get a } b_o \text{ to } b_r \text{ ratio of 10. Thus,}$$

ferricytochrome *c* absorbed more strongly onto the surface than is ferrocyanochrome *c*. This value is a little bit larger than previous studies which showed that the stabilization of ferricytochrome *c* is three to seven times larger than that of ferrocyanochrome *c*, so this may not be the only factor causing the negative shift of formal potential.

Murguida and Hildebrandt have evaluated the potential drop across a SAM. The formal potential was found to shift to more negative values as the thickness of the SAM increases, with a net change of 41 mV from alkane chain C<sub>2</sub> to C<sub>16</sub>. After subtraction of a potential drop of 41 mV, the relative strength of adsorption of ferricytochrome *c* and ferrocyanochrome *c* was

reevaluated, and the ratio  $b_O$  to  $b_R$  is 2. These comparisons show that the observed potential shifts are reasonable in sign and size and agree reasonably well with the work of others.

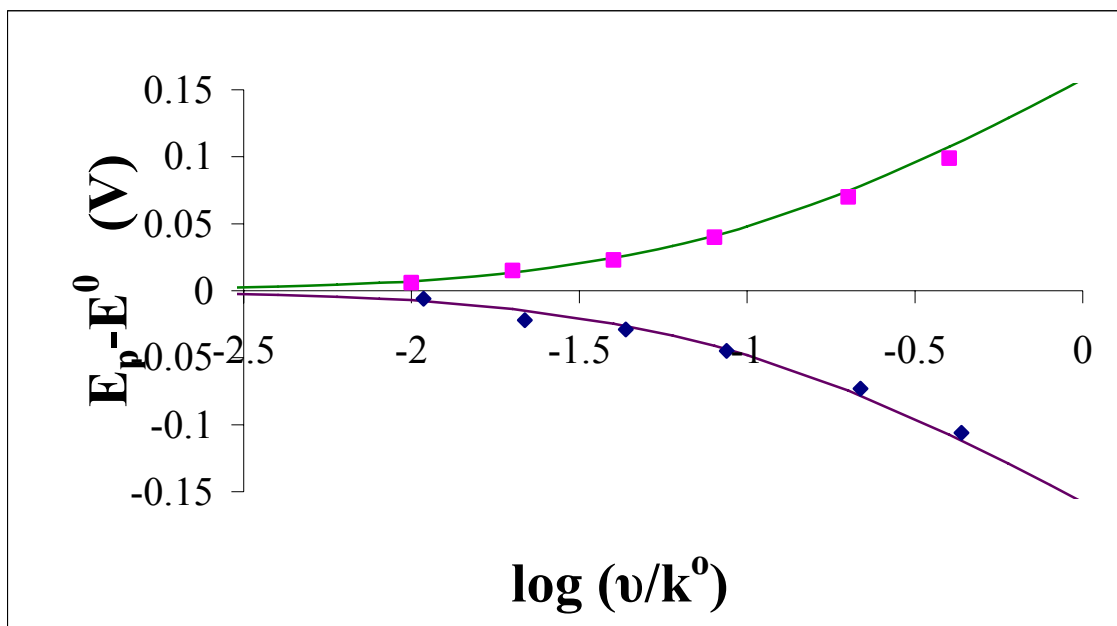
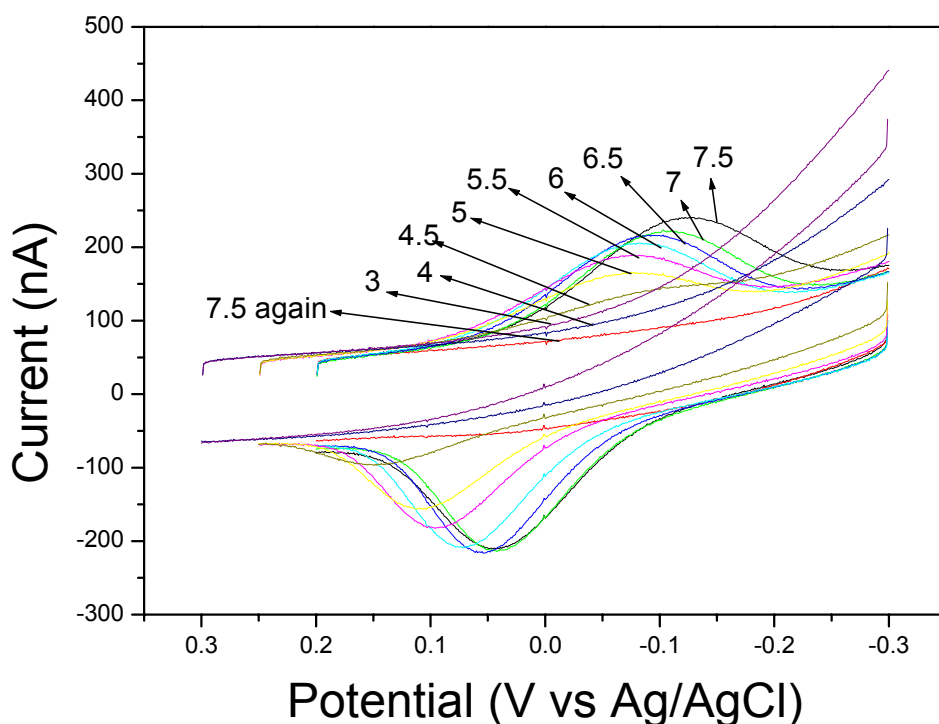


Figure 4. Fitting of experimental peak separation as a function of scan rate to Butler-Volmer model. The data are from Figure 3.

As the potential scan rate increases, the peak-peak separation becomes larger and FWHHs for both cathodic and anodic peaks become broader. Thus, the redox reaction becomes quasi-reversible. The standard electrochemical rate constant  $k^0$  can be extracted from the relationship between scan rate and peak separation by fitting the curve to the model built by Butler and Volmer. Fig 4 shows the fitting result with  $k_f^0 = 2.5$  Hz and  $k_b^0 = 2.2$  Hz which matches well with the results of cytochrome *c* covalently attached to C16 acid and C14-OH mixed SAM obtained by Yue.<sup>39</sup> Because the electron transfer rate is slow, only at low scan rate could a reversible reaction be achieved, which corresponds to the analysis made before.

The effect of pH on the electrochemical reduction of ferricytochrome *c* is shown in figure 5. As the pH decreases, the peak currents strongly decrease. At pH = 4, the Faradaic peak current drops almost to zero. It is evident from the electrochemical data shown in Fig 6 that the

amount of active His/Met-ligated protein decreases from 100% to almost zero upon decreasing the pH. The percentage of active His/Met-ligated protein at pH 6, 5 and 4 was determined to be 91%, 56% and 5% respectively by integrating the charge under the peak.



*Figure 5. Cyclic voltammograms of covalently attached Cyt C on mixed carboxylic SAM ( 40% 16-MHDA and 60% 14-MTOH) at different pH. Scan rate: 500 mV/s.*

A similar transition caused by pH changes has been examined by Cheng and co-workers.<sup>12</sup> On the basis of optical absorption spectrometry, they reported a surface-assisted acid-induced protein unfolding. The Soret absorption peak is observed to shift from 409 to 397 nm as the pH of the solution decreases from 10 to 2.5, where a sharp transition is found between pH 2.5 and 3.0.

Fig. 6 illustrates the peak current dependence on pH. Compared with the solution results, the peak currents of surface immobilized cytochrome *c* decrease steadily with solution pH ranging from 7.5 to 3. The midpoint of the transition is found between pH 4.5 and 5 which is 2 units higher than that in solution. This phenomenon indicates that cytochrome *c* immobilized on the surface is less stable and more vulnerable to the pH effect. This result correlates well with the  $pK_a = 5.2$  obtained by protonation of Histidine residue in the peptide chain.<sup>9</sup> We attribute the sudden current decrease to the unfolding of the cytochrome *c*, in particular changes in the heme pocket and the exposure of the heme to solvent.

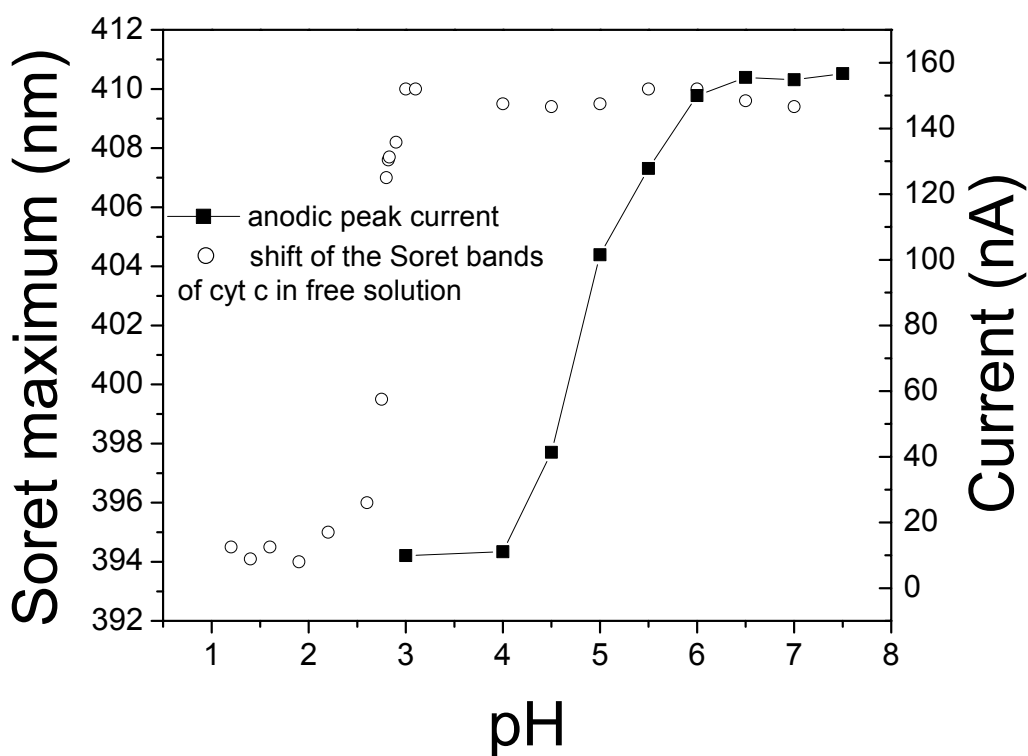


Figure 6. Variation of the peak currents during the acid titration. The ■ points represent anodic peak currents, and the ○ points represent the shift of the Soret bands of cyt *c* in free solution obtained by Cheng<sup>4</sup>

Other denaturants, like urea and pyridine give similar behaviors, as observed for pH. In cyclic voltammetric experiments, voltammograms were recorded by continuously increasing the urea concentration in pH 7 phosphate buffer. Fig 7 illustrates the peak current dependence on concentration of the urea. The amount of active His/Met-ligated protein decreases from 100% to almost zero upon increase in the denaturant concentration from 0 M to 10 M urea. Similar findings were also reported by Russell<sup>1</sup> and Fedurco<sup>9</sup>. In 9 M urea, the spectrum of cytochrome *c* in the visible region closely resembles that of the bis-His cytochrome *c* at pH 7.0, consistent with the replacement of the axial Met-80 by a His ligand.

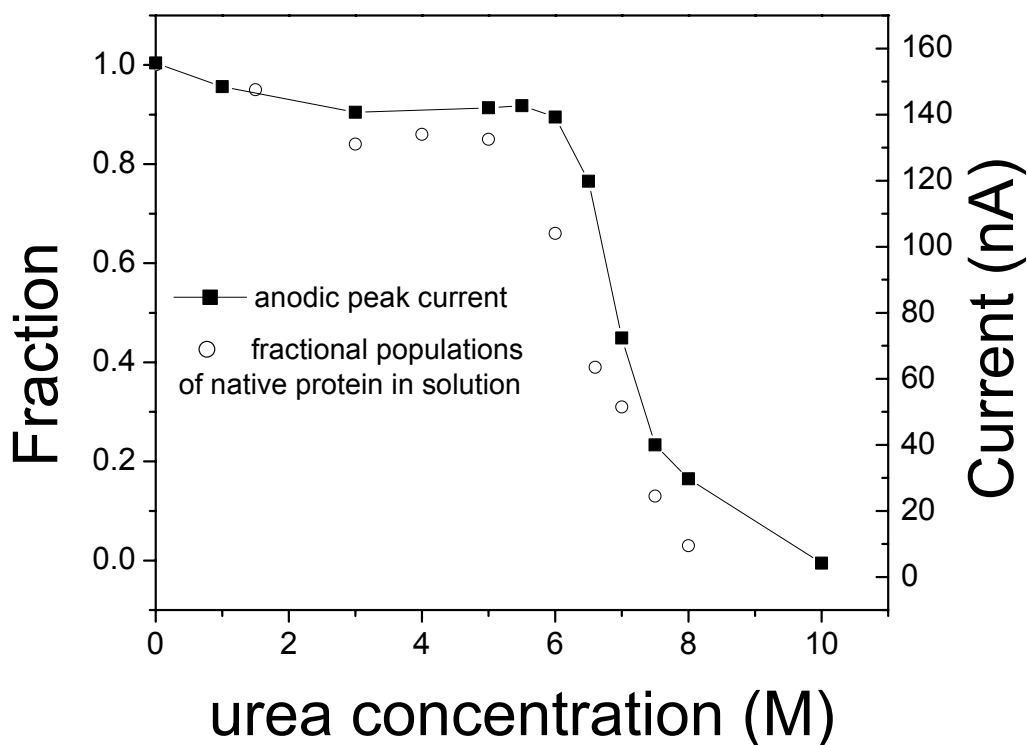


Figure 7. Variation of the peak currents by increasing the urea concentration in pH 7 phosphate buffer. The cyclic voltammograms of covalently attached Cyt C on mixed carboxylic SAM ( 40%

16-MHDA and 60% 14-MTOH ) were recorded at the scan rate: 500 mV/s. The ■ points represent anodic peak currents, and the ○ points represent the fractional populations of native protein in solution obtained by Russell.<sup>1</sup>

To mimic the biological environment of cytochrome *c*, cardiolipin containing liposomes have been used to bind cytochrome *c*. Cytochrome *c* is positively charged at neutral pH and the inner mitochondrial membrane contains a large fraction of negatively charged phospholipid, cardiolipin. So cytochrome *c* interacts electrostatically with the inner membrane in the mitochondria. It has been shown that once bound to cardiolipin, cytochrome *c* will change its conformation and its chemical reactivity.<sup>25</sup> Kagan's group discovered that cytochrome *c* plays a critical role in early apoptosis as a cardiolipin-specific oxygenase to produce cardiolipin hydroperoxides required for the release of proapoptotic factors. They found that at low ionic strength and high CL/cyt *c* ratio, peroxidase activity of CL/cyt *c* complex was increased > 50 times vs soluble cytochrome *c*.<sup>48</sup> So the voltammetric behavior of CL/cyt *c* complex was studied here (Fig 8).

In this experiment, cytochrome *c* was covalently attached onto the mixed carboxylic SAM in pH 7.0. After that, the electrode was placed into a solution with 2 mM cardiolipin contained in liposomes and 10 mM phosphate buffer. Voltammograms were recorded at different times after its immersion into the liposome solution. Both the anodic and cathodic peaks around 0 V, attributed to the redox peaks of native cytochrome *c*, decreased while another couple of peaks started to increase as time elapsed. The  $E_{pc}$  and  $E_{pa}$  for the newly appearing cathodic peak and anodic peak are -0.43 V and -0.03 V respectively, which was attributed to the bis-His-Fe(III)/bis-His-Fe(II) couple. The peak-peak separation is about 400 mV, that is to say, this process is irreversible at the scan rate 30 V/s. Changing scan rate does not help the reversibility of this redox reaction. If the scan rate goes too low (slower than 1 V/s for this case), the faradaic current

will be buried in the charging current and cannot be distinguished. This is consistent with the results of Fedurco et al who observed a new cathodic peak appearing at ca. -0.2 V vs NHE and an anodic peak coincided with reoxidation of the His/Met-Fe(II) to His/Met-Fe(III) at ca. +0.27 V vs NHE by addition of 7 M urea.<sup>8</sup>

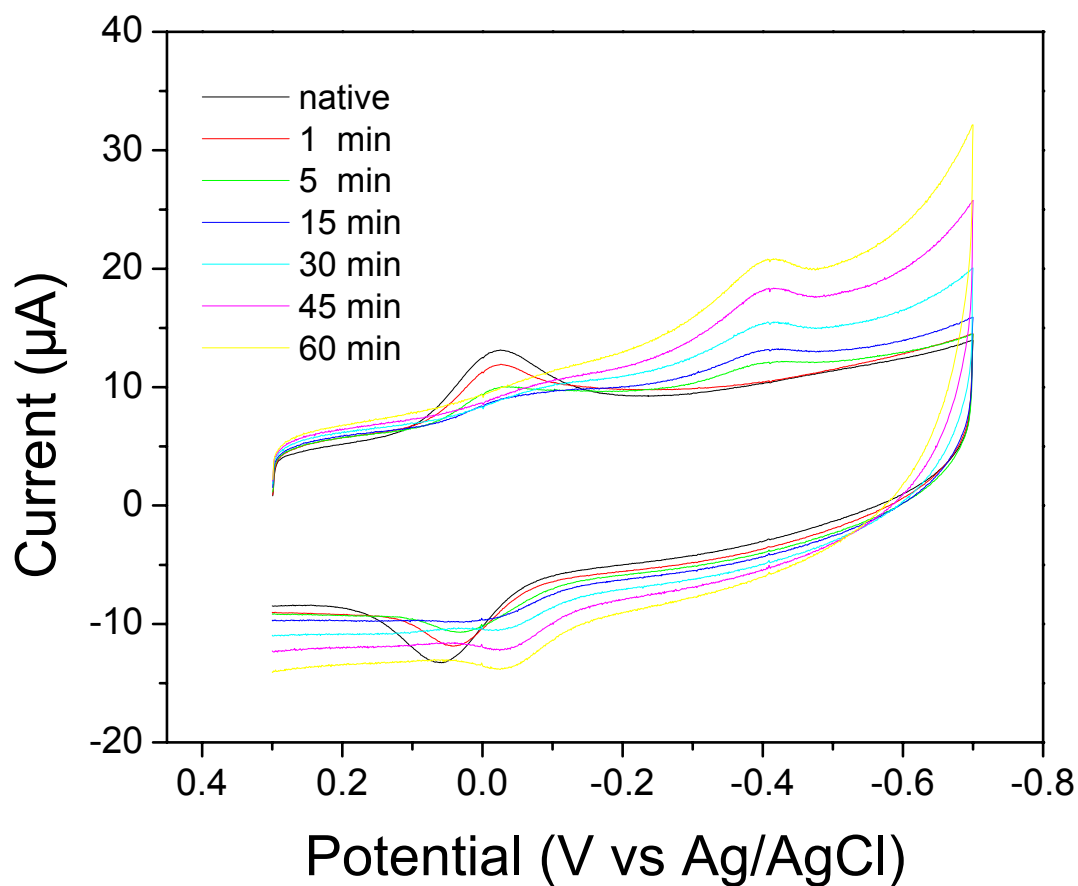


Figure 8. Time dependent cyclic voltammograms of CL/cyt c complex immobilized onto mixed carboxylic SAM. Solution condition: 2 mM TOCL/ 2 mM PC liposome in 10 mM pH 7.0 phosphate buffer. Scan rate: 30 V/s

## 4.2 CYTOCHROME *C* AS PEROXIDASE

When cytochrome *c* is in its native state, the heme pocket is wrapped by the peptide chain and protected from the solvent, even though it is located near the protein edge. So far, we have addressed how cytochrome *c* can be unfolded by decreasing the pH value or increasing a denaturant's concentration. When cytochrome *c* is unfolded by lowering the pH, the heme pocket loses its axial ligands, causing the heme pocket to unwrap and exposing the heme to solvent molecules. Easy access to the heme pocket can facilitate the hydroperoxide catalyzing reaction.

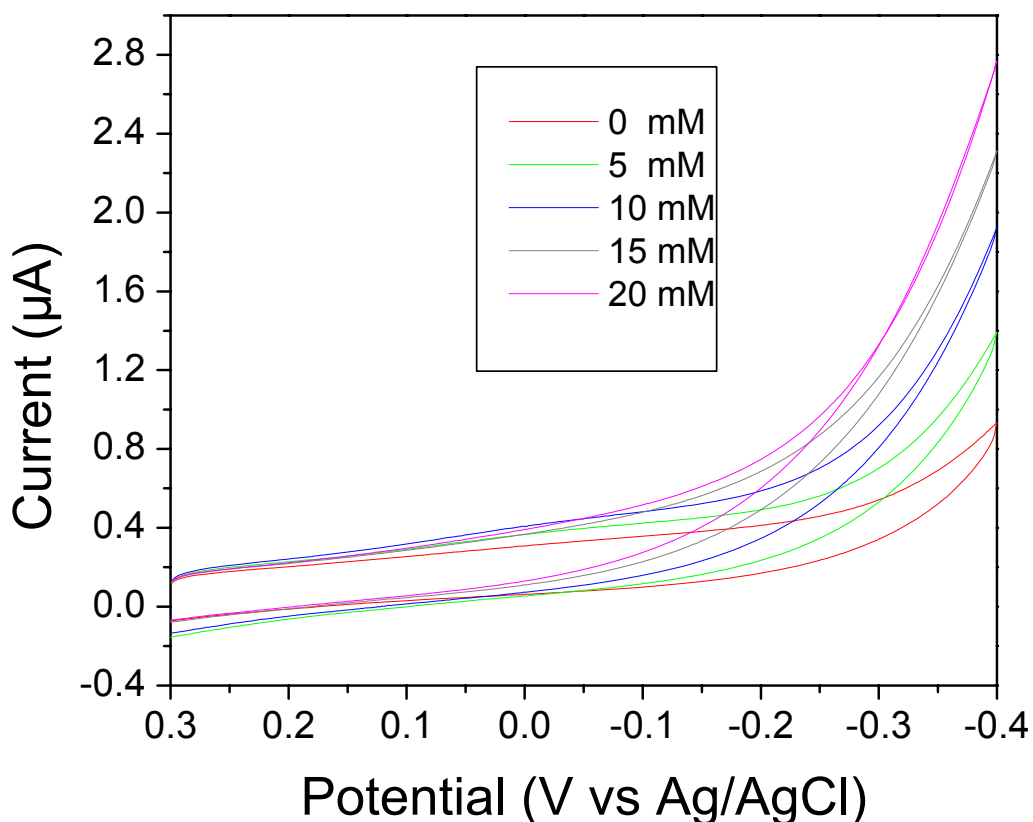
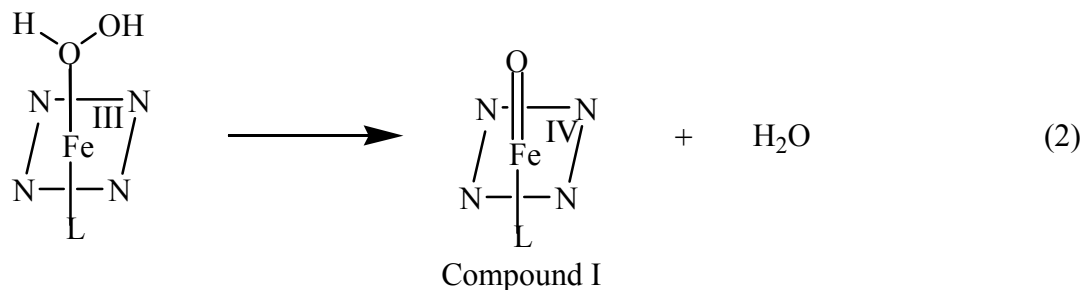
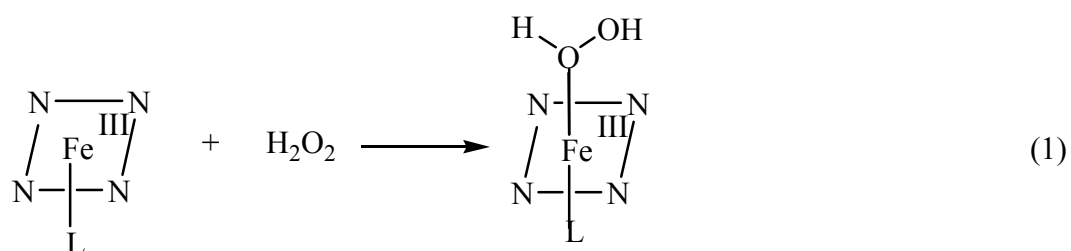
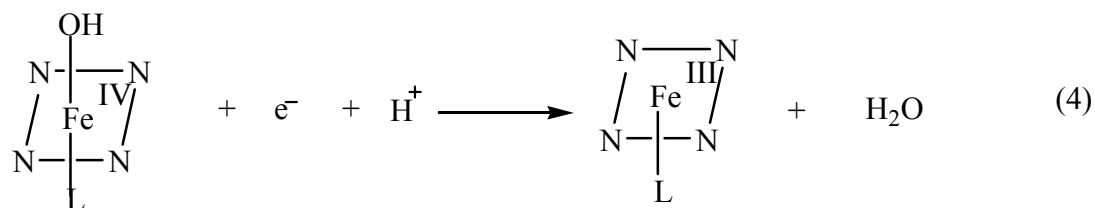
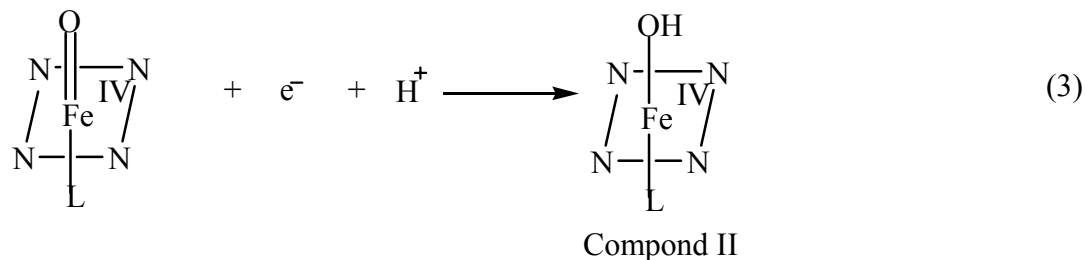


Figure 9. Cyclic voltammograms of different concentration  $H_2O_2$  in pH 3, 1M phosphate buffer, at a gold electrode modified by cytochrome *c*. Scan rate: 500 mV/s

Fig. 9 shows the voltammetric behavior of the cytochrome *c* modified gold electrode in different concentration of H<sub>2</sub>O<sub>2</sub> at pH 3. After adding H<sub>2</sub>O<sub>2</sub> into the buffer solution, a great enhancement of current was observed, and the current was quite stable even after several continuous scans. Moreover, the current increased with the concentration of H<sub>2</sub>O<sub>2</sub>. A similar phenomenon was observed for microperoxidase-11 (MP-11), which consists of the active-site of cytochrome *c* obtained by proteolytic digestion of heme protein, by other groups.<sup>49,50</sup> The electrocatalytic current rises at ca. 0.2 V with respect to Ag/AgCl (sat. KCl solution). It should be noted that the electrocatalytic current for the reduction of H<sub>2</sub>O<sub>2</sub> in aqueous solution is observed much higher than the redox potential  $E^{0'} = -0.398$  V vs SCE of MP-11 itself. The reason for this potential shift is hypothesized to result from the formation of the Fe(IV) intermediate species in the presence of H<sub>2</sub>O<sub>2</sub>. The reducibility of the high-valency compound at +200 mV vs Ag/AgCl is consistent with the redox potentials for the Compound I/Compound II and Compound II/ Fe(III) couples of horseradish peroxidase, which are more positive than +900 mV vs NHE at pH 6.4.<sup>51</sup> So the possible reaction mechanism has been suggested to be:<sup>52,53</sup>





If the sixth coordination position of the heme protein is vacant or easily replaceable, peroxidase reactions proceed via occupancy or replacement of the sixth ligand by hydrogen peroxide to give an Fe(III) hydroperoxide intermediate (step 1). This step involves the heterolytic cleavage of the oxygen-oxygen bond to produce a two-electron-oxidized oxene species, which is often the rate determining step. Loss of water yields an oxoferryl species that can be observed spectroscopically and is generically known as Compound I (step 2). In acidic solution, Compound I accepts an electron to form another intermediate named Compound II (step 3). A second one-electron transfer returns the enzyme to the original state (step 4).

Fig. 10. shows a control experiment for a gold electrode coated with mixed carboxylic SAM in the presence of different concentration of H<sub>2</sub>O<sub>2</sub> at pH 3. After adding H<sub>2</sub>O<sub>2</sub> into the buffer solution, the voltammograms remain almost intact and are independent of the concentration of H<sub>2</sub>O<sub>2</sub>. The slight change of the current may be caused by the non-specific adsorption of oxygen produced by the chemical dissociation of H<sub>2</sub>O<sub>2</sub>. The absorbed oxygen will slightly change the double layer of the SAM and lead to the change of capacitance and affect the charging current. The concern that the increasing current in Fig.9 arises from oxidation of the SAM by H<sub>2</sub>O<sub>2</sub> can be excluded by this control experiment. In fact, the gold-sulfur bond formed

between alkanethiol and gold is pretty stable throughout the potential range of 1.0V to -1.4V versus Ag/AgCl before being oxidatively or reductively desorbed.

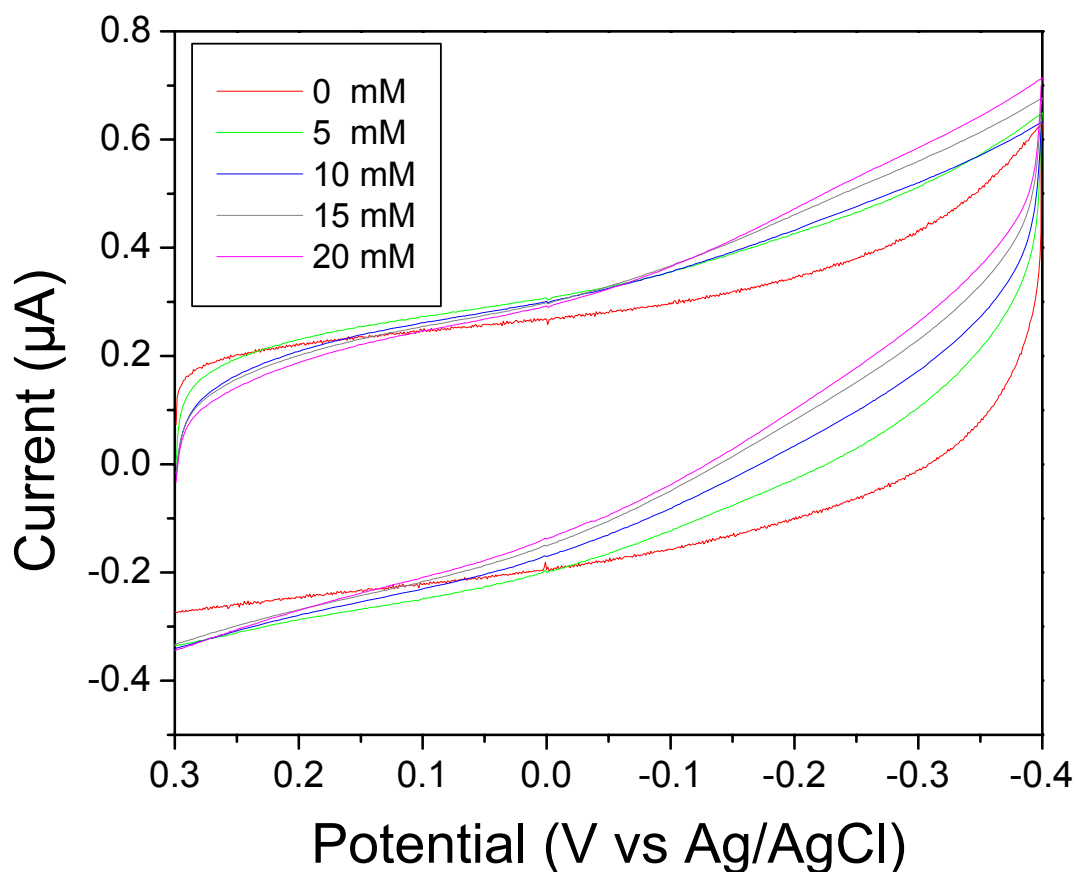
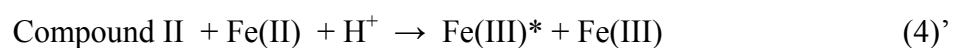


Figure 10. Cyclic voltammograms of different concentration  $H_2O_2$  in pH 3, 1 M phosphate buffer, at a gold electrode coated with mixed carboxylic SAM. Scan rate: 500 mV/s

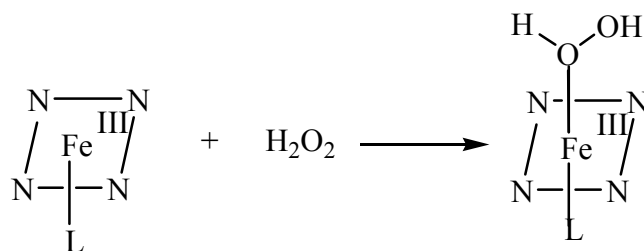
The electrocatalytic current in Fig. 9. seems to rise from ca. 0.1 V, but from the control experiment, we can observe similar change of current from ca. 0.1 V too. After background correction using the two data sets, the true rise of electrocatalytic current is from ca. -0.2V, which is consistent with the redox potential for the His-Fe(III)-H<sub>2</sub>O /His-Fe(II) couple of urea

denatured cytochrome *c*. Therefore, the suggested peroxidase reaction mechanism of MP-11 may not be applicable for denatured cytochrome *c* as peroxidase.

Here we suggest a plausible mechanism. For the denatured cytochrome *c* as peroxidase, the first two steps are the same as the mechanism of MP-11, which involves the heterolytic cleavage of the oxygen-oxygen bond to produce an Fe(III) hydroperoxide intermediate and loss of water to yield Compound I. The third and fourth steps involve electron transfer from ferrocyanochrome *c* to the oxidized sites of Compound I and Compound II, forming the product ferricytochrome *c*. These two steps involve complex formation between peroxidase and ferrocyanochrome *c* and both steps are essentially irreversible. The enhancement of current rising from ca -0.2V comes from reducing denatured cytochrome *c* His-Fe(III)-H<sub>2</sub>O to His-Fe(II) coupled with the continuous supply of ferricytochrome *c* by steps 3 and 4. This mechanism is similar to the cytochrome *c* P450 mode adopted by yeast cytochrome *c* peroxidase.<sup>54</sup> Osman et al. demonstrated that it was possible to separate the peroxidase and P450 activities by the addition of ascorbate to the catalytic system.<sup>55</sup>



Integration of the charge under the curves give us the amount of consumed H<sub>2</sub>O<sub>2</sub> in each cycle. For the reaction,



the reaction rate is described as,

$$\frac{d[H_2O_2]}{dt} = k[H_2O_2][Cyt\ c].$$

Plotting the  $H_2O_2$  reaction rates versus the  $H_2O_2$  concentrations, with the known concentration of cytochrome  $c$  immobilized on the surface, we can determine the rate constant  $k$  to be  $2.08 \times 10^4 \text{ cm}^2 \cdot \text{mol}^{-1} \cdot \text{s}^{-1}$  (Fig 11).

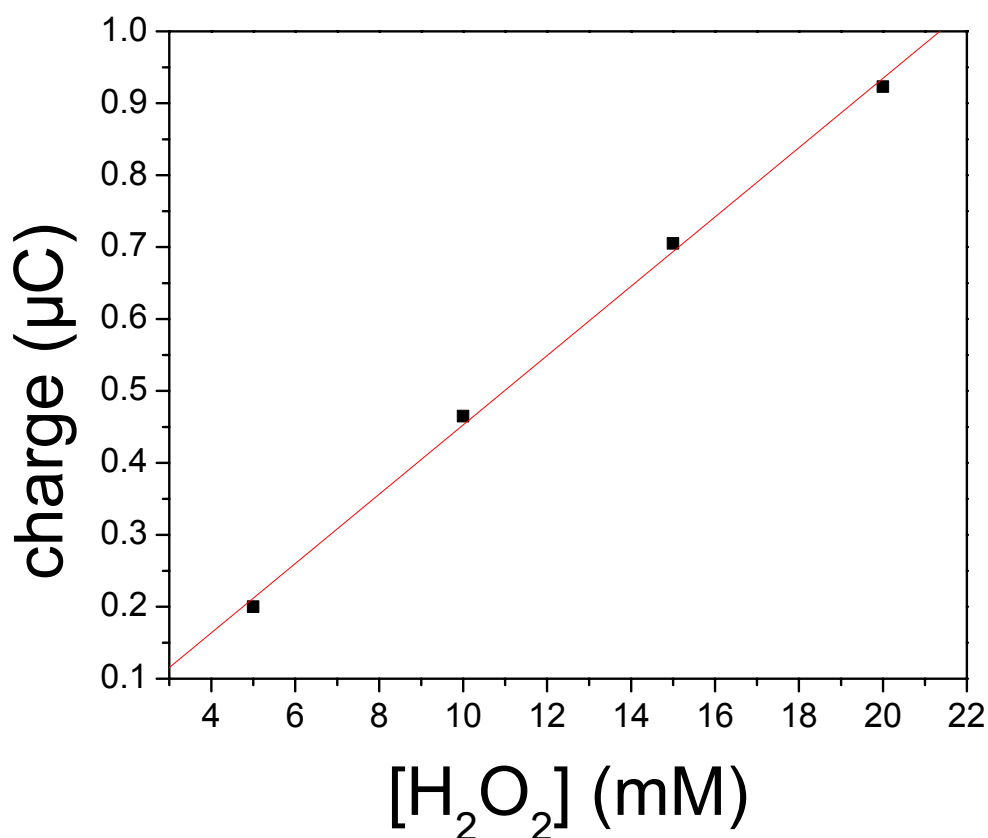


*Figure 11. Charge dependence on concentration of  $H_2O_2$ .*

We have shown that once bound to cardiolipin, cytochrome  $c$  will change its conformation and result in the change of chemical reactivity. Interaction of cytochrome  $c$  with cardiolipin containing liposome induces the breaking of the Fe-S (Met<sub>80</sub>) bond so that the native heme

structure has been changed. At this point,  $H_2O_2$  is able to access the heme catalytic site and trigger peroxidase activity. Several types of direct measurements of peroxidase activity using chemiluminescence, fluorescence and the electron paramagnetic resonance (EPR) responses confirmed that the CL/cyt *c* complex is an active peroxidase, neither cytochrome *c* alone nor cardiolipin containing liposome displayed any comparable peroxidase activity.<sup>48</sup>

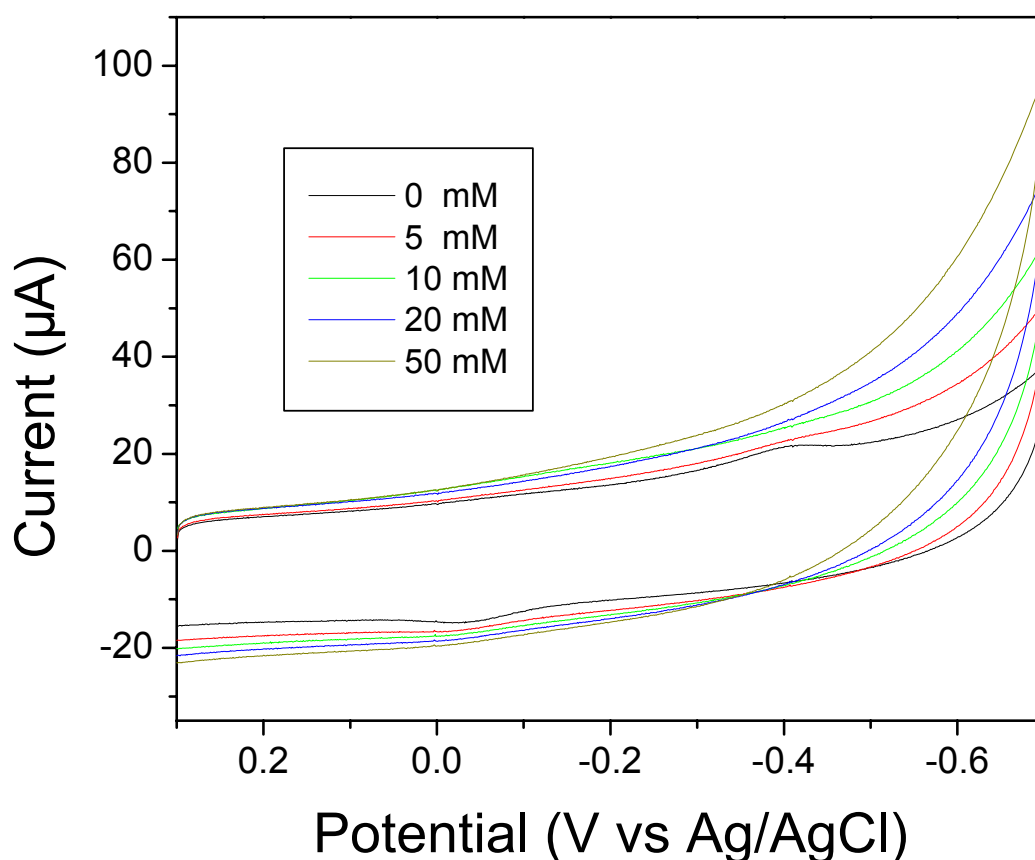


*Figure 12. Cyclic voltammograms of different concentration  $H_2O_2$  in pH 7, 10 mM phosphate buffer, at a gold electrode modified by liposome denatured cytochrome *c*. Scan rate: 30 V/s*

Here we checked the peroxidase activity of denatured cytochrome *c* by the electrochemical method. After the complete denaturation of cytochrome *c* by exposure to the liposome, the

electrode coated with denatured cytochrome *c* was placed into different concentrations of H<sub>2</sub>O<sub>2</sub>. Fig. 12 shows the cyclic voltammograms of gold electrodes coated with denatured cytochrome *c* in different concentrations of H<sub>2</sub>O<sub>2</sub> in 10 mM phosphate pH 7 buffer. The electrocatalytic currents increase with the concentration of H<sub>2</sub>O<sub>2</sub>. The evidence for a peak current around ca. -0.43 V disappears as the concentration increases but the current keeps increasing as the potential goes negative. This behavior is characteristic of an electrochemical reaction coupled with a catalytic reaction called EC reaction. So cytochrome *c* bound to CL-containing liposome acts as a peroxidase.

### 4.3 OXYGEN REACTION

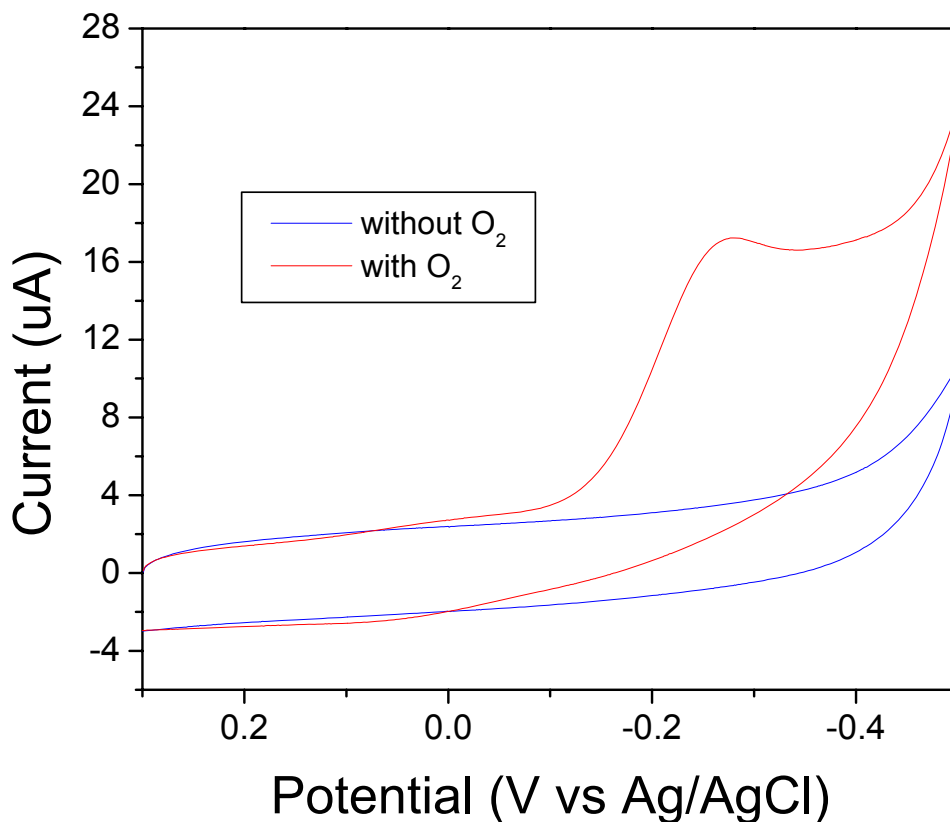


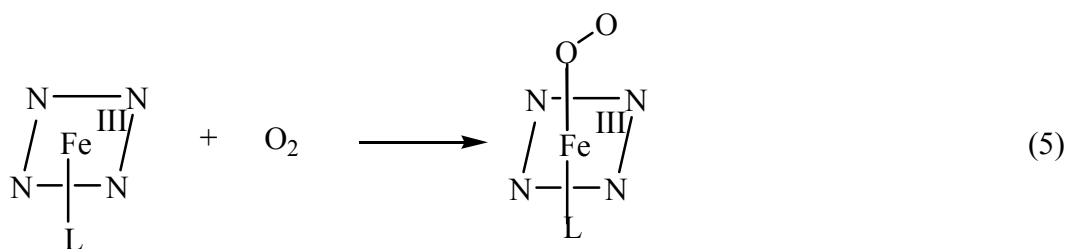
*Figure 13. Cyclic voltammograms of gold electrode modified by denatured cytochrome *c* in 10 mM pH 3 phosphate buffer with or without O<sub>2</sub>. Scan rate: 1 V/s*

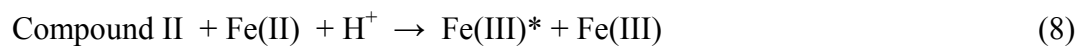
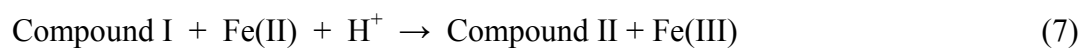
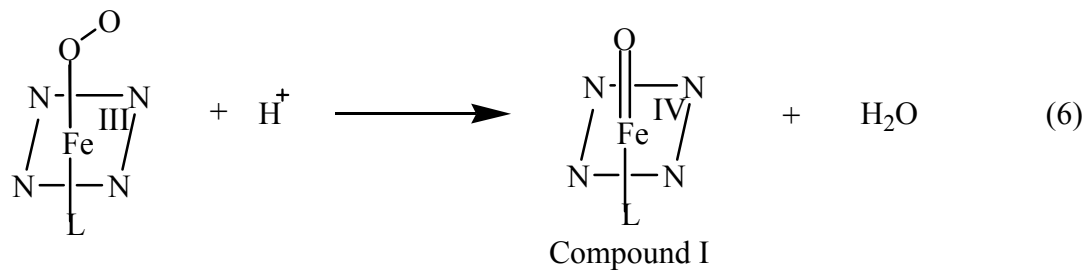
Another interesting phenomenon we found for denatured cytochrome *c* is the reaction with oxygen. If the solution contains oxygen, we can see a huge increase of cathodic current with a peak potential at ca. -0.28 V (Fig. 13). In fact, it was noted that the voltammogram recorded on a silver electrode for the urea denatured cytochrome *c* is very sensitive to traces of molecular oxygen.<sup>8</sup> There are three possible reasons:

(1) the direct reduction of oxygen.  $E^{0'} = 0.695$  V vs NHE for the reaction  $O_2 + 2H^+ + 2e \rightleftharpoons H_2O_2$  and  $E^{0'} = 1.229$  V vs NHE for the reaction  $O_2 + 4H^+ + 4e \rightleftharpoons 2H_2O$ , while the observed peak potential is ca. -0.28 V. For a control experiment (Fig. 10), voltammograms were recorded on a gold electrode coated with a mixed carboxylic SAM but without cytochrome *c* in 10 mM pH 3 phosphate buffer purging with oxygen. We did not see any peak in this case so that I can exclude the possibility (1).

(2) Reduction of unfolded cytochrome *c* mediated by oxygen. Oxygen is a natural mediator and it plays a very important role in the glucose oxidase catalytic reaction. This possibility could be checked by replacing the oxygen with another mediator to see if we can observe the cathodic current or not.

(3) Reduction of the complex of cytochrome *c* and oxygen with subsequent formation of compound I and oxidation of the protein. Here, we are trying to interpret this phenomenon by the cytochrome P-450 mechanism. Like the interaction of  $H_2O_2$  with denatured cytochrome *c*, oxygen may interact with denatured cytochrome *c* to form a complex. In acidic condition, this complex is converted to compound I. Compound I is highly oxidative with a redox potential around 900 mV vs NHE, so it will oxidize the ferrocycytochrome *c* to ferricytochrome *c*. The cathodic current results from reducing denatured cytochrome *c* His-Fe(III)- $H_2O$  to His-Fe(II) couple with the continuous supply of ferricytochrome *c*. How molecular oxygen will interact with denatured cytochrome *c* and the detail mechanism is under study.





## 5.0 CONCLUSION

The present work uses a chemically modified gold ball electrode to explore how the unfolding of cytochrome *c* affects its electrochemistry. Covalently attaching cytochrome *c* onto mixed carboxylic acid and hydroxyl terminated SAM prevents the loss of cytochrome *c* during the experiment. The amount of immobilized cytochrome *c* onto the SAM is the order of pmol/cm<sup>2</sup> with the surface coverage 7%~10%. The formal potential for the native Fe(III)/Fe(II) is found to be  $0.203 \pm 0.002$  V vs NHE on the mixed carboxylic SAM, which is 60 mV more negative than the formal potential of native cytochrome in solution. The potential drop across the SAM and the relative strength of adsorption of ferricytochrome *c* and ferrocyanochrome *c*, can explain this shift.

Cyclic voltammetry allows one to monitor the redox reaction during the unfolding process of cytochrome *c*. The effect of pH on cytochrome denaturation is irreversible. As the pH decreases, the peak currents strongly decrease. At pH = 4, the Faradaic peak current drops almost to zero. The amount of active His/Met-ligated protein at pH 6, 5 and 4 was determined to be 91%, 56% and 5%, respectively, by integrating the charge under the peak. The midpoint of the transition is found between pH 4.5 and 5 which is two units higher than the situation happening in the solution case. This phenomenon indicates that cytochrome *c* immobilized on the surface is less stable and more vulnerable to the pH effect. The currents do not recover when

the pH value is reversed. Other denaturants, like urea and pyridine exerted similar behaviors as pH.

When cytochrome *c* is in its native state, the heme pocket is wrapped by the peptide chain and protected from the solvent. When cytochrome *c* is unfolded by lowering the pH, the heme pocket loses its integrity and unwraps, exposing the heme to solvent molecules. Easy access of the heme pocket facilitates the peroxidase activity. After adding H<sub>2</sub>O<sub>2</sub> into the buffer solution, a great enhancement of current was observed, and the current was quite stable even after several continuous scans. Moreover, the current increased with the concentration of H<sub>2</sub>O<sub>2</sub>. A cytochrome P-450 type catalysis mechanism was suggested.

To mimic the biological environment of cytochrome *c*, an electrode coated with cytochrome *c* was placed into 2 mM cardiolipin containing liposome solution in 10 mM phosphate buffer. Both the anodic and cathodic peaks around 0 V attributed to the redox peaks of native cytochrome *c* decreased while another couple of peaks assigned to the denatured cytochrome *c* started to increase as time lapsed.

Peroxidase activity of denatured cytochrome *c* binding with liposome was checked by voltammetry. The result showed a characteristic electrochemical reaction couple with catalytic reaction called EC reaction. So cytochrome *c* bound to CL-containing liposome acts as a peroxidase that selectively catalyzed CL peroxidation. This reactivity could contribute to the outer mitochondrial membrane permeation, release of cytochrome *c* into the cytosol and completion of the apoptotic program.

Finally, denatured cytochrome *c* may serve as an oxygenase to bind with O<sub>2</sub> forming a complex. When the solution contains oxygen, a huge increase of cathodic current with the peak

potential at ca. -0.28 V was observed. Three possible reasons were given. But how molecular oxygen will interact with denatured cytochrome *c*, and its detailed mechanism is under study.

## 6.0 FUTURE PLANS

To check the proposed mechanism for denatured cytochrome *c* as a peroxidase, the oxidized form of a species with its redox potential between ca 0.4 V (the potential at which electrocatalytic current starts to rise for MP-11) and ca. 0 V ( the potential at which electrocatalytic current starts to rise for denatured cytochrome *c*) vs NHE could be added into the buffer solution. e.g.  $\text{Fe}(\text{CN})_6^{3-}/\text{Fe}(\text{CN})_6^{4-}$ ,  $E^{0'} = 0.3610$  ;  $\text{Ru}(\text{NH}_3)_6^{3+}/\text{Ru}(\text{NH}_3)_6^{2+}$ ,  $E^{0'} = 0.10$ . The formed compound I by interaction of  $\text{H}_2\text{O}_2$  with denatured cytochrome *c* will preferably oxidize the added species instead of ferrocycytochrome *c*. So we can expect the suppression of rising current at ca. -0.2 V vs Ag/AgCl.

To understand the interaction of  $\text{O}_2$  with denatured cytochrome *c*, we are seeking another mediator instead of  $\text{O}_2$ . If we can still observe the cathodic current,  $\text{O}_2$  just plays a role as mediator to facilitate the denatured cytochrome *c* redox reaction, and vice versa.

After cytochrome *c* was denatured, it was sensitive to the ionic strength. It has been noted that under high ionic strength, cytochrome *c* may refold into a globular molten state.  $\text{NaClO}_4$  may be applied to adjust the ionic strength of the solution. Both the dependence of voltammetric behavior and the change in peroxidase activity with ionic strength could be studied.

The Quartz Crystal Microbalance (QCM) is an extremely sensitive mass sensor, capable of measuring mass changes in the nanogram range. QCMs are piezoelectric devices fabricated of a thin plate of quartz with electrodes affixed to each side of the plate. During the experiment of

cytochrome *c* binding with liposome, we observed the decreasing native peaks ca. 0V and another increasing peaks. But we do not completely understand this process because the denaturation process is so mild and slow or because the liposome is slowly depositing on the electrode surface. We are able to utilize the QCM to monitor the mass change at the electrode surface. When liposome deposits onto the electrode surface, the quartz oscillating frequency will change with the mass of depositing material. Observing the frequency change allows us to know the denaturation process better.

Resonance Raman spectroscopy has been demonstrated to be especially useful to study the conformation of the heme proteins. On the basis of this knowledge, four folding intermediates of ferric cytochrome with different heme coordination states were identified: (1) the native form in which His 18 and Met 80 are the axial ligands. (2) a bis-his form where Met 80 is replaced by His 26 or His 33. (3) a histidine-water form where Met 80 is replaced by a water molecule. (4) a five-coordinated form where both the Met 80 and His 18 iron bonds are broken and a water molecule is ligated to the heme as the single axial ligand. Through the resonance Raman spectra, we can observe the conformation of protein in different solution conditions, which will help us understand the denaturation process better.

## APPENDIX A

The Langmuir isotherms for two adsorbed species are:

$$\Gamma_o(t) = \frac{\beta_o \Gamma_{o,s} C_o(0,t)}{1 + \beta_o C_o(0,t) + \beta_R C_R(0,t)} \quad 3-1$$

$$\Gamma_R(t) = \frac{\beta_R \Gamma_{R,s} C_R(0,t)}{1 + \beta_o C_o(0,t) + \beta_R C_R(0,t)} \quad 3-2$$

The general flux equation is:

$$-\frac{\partial \Gamma_o(t)}{\partial t} = \frac{\partial \Gamma_R(t)}{\partial t} = \frac{i}{nFA} = \left[ \frac{\partial \Gamma_o(t)}{\partial E} \right] \nu \quad 3-3$$

$$\Gamma_o(t) + \Gamma_R(t) = \Gamma^* \quad 3-4$$

From 3-1 and 3-2,

$$\frac{\Gamma_o(t)}{\Gamma_R(t)} = \frac{\beta_o \Gamma_{o,s} C_o(0,t)}{\beta_R \Gamma_{R,s} C_R(0,t)} = \frac{b_o C_o(0,t)}{b_R C_R(0,t)} \quad 3-5$$

If the reaction is Nernstian,

$$\frac{C_o(0,t)}{C_R(0,t)} = \exp \left[ \left( \frac{nF}{RT} \right) (E - E^{0'}) \right] \quad 3-6$$

Then 3-5 yields,

$$\frac{\Gamma_o(t)}{\Gamma_R(t)} = \left( \frac{b_o}{b_R} \right) \exp \left[ \left( \frac{nF}{RT} \right) (E - E^{0'}) \right] \quad 3-7$$

Combining 3-3, 3-4, and 3-7, the i-E curve is obtained:

$$i = \frac{n^2 F^2 \nu A \Gamma^* (b_O / b_R) \exp[(nF / RT)(E - E^{0'})]}{RT \{1 + (b_O / b_R) \exp[(nF / RT)(E - E^{0'})]\}^2} \quad 3-8$$

The location of  $E_p$  with respect to  $E^{0'}$  depends on the relative strength of adsorption of O and R according to the principles of stabilization. If  $b_O = b_R$ ,  $E_p = E^{0'}$ . If O is adsorbed more strongly ( $b_O > b_R$ ), the wave is displaced toward negative potentials, beyond the position where the reversible wave of a diffusing species would occur. For this reason, it is named a postwave. If R is adsorbed more strongly ( $b_R > b_O$ ), the wave occurs at more positive potentials than  $E^{0'}$  and is called a prewave.

## BIBLIOGRAPHY

- (1) Russell, B. S.; Melenkivitz, R.; Bren, K. L. *Proceedings of the National Academy of Sciences of the United States of America* **2000**, *97*, 8312-7.
- (2) Zhu, H.; Snyder, M. *Current opinion in chemical biology* **2003**, *7*, 55-63.
- (3) Lee, Y.-S.; Mrksich, M. *Trends in biotechnology* **2002**, *20*, S14-8.
- (4) Cheng, Y. Y.; Lin, S. H.; Chang, H. C.; Su, M. C. *Journal of Physical Chemistry A* **2003**, *107*, 10687-10694.
- (5) Love, J. C.; Estroff, L. A.; Kriebel, J. K.; Nuzzo, R. G.; Whitesides, G. M. *Chemical Reviews (Washington, DC, United States)* **2005**, *105*, 1103-1169.
- (6) Scott, R. A.; Mauk, A. G.; Editors *Cytochrome c: A Multidisciplinary Approach*, 1996.
- (7) Yeh, S.-R.; Han, S.; Rousseau, D. L. *Accounts of Chemical Research* **1998**, *31*, 727-736.
- (8) Fedurco, M.; Augustynski, J.; Indiani, C.; Smulevich, G.; Antalik, M.; Bano, M.; Sedlak, E.; Glascock, M. C.; Dawson, J. H. *Journal of the American Chemical Society* **2005**, *127*, 7638-7646.
- (9) Fedurco, M.; Augustynski, J.; Indiani, C.; Smulevich, G.; Antalik, M.; Bano, M.; Sedlak, E.; Glascock, M. C.; Dawson, J. H. *Biochimica et Biophysica Acta, Proteins and Proteomics* **2004**, *1703*, 31-41.
- (10) Yeh, S. R.; Rousseau, D. L. *Nature structural biology* **1998**, *5*, 222-8.
- (11) Bixler, J.; Bakker, G.; McLendon, G. *Journal of the American Chemical Society* **1992**, *114*, 6938-9.
- (12) Cheng, Y.-Y.; Chang, H.-C.; Hoops, G.; Su, M.-C. *Journal of the American Chemical Society* **2004**, *126*, 10828-10829.

- (13) Battistuzzi, G.; Borsari, M.; Sola, M. *European Journal of Inorganic Chemistry* **2001**, 2989-3004.
- (14) Goto, Y.; Calciano, L. J.; Fink, A. L. *Proceedings of the National Academy of Sciences of the United States of America* **1990**, *87*, 573-7.
- (15) Evans, P. A.; Radford, S. E. *Current Opinion in Structural Biology* **1994**, *4*, 100-6.
- (16) Roder, H.; Elove, G. A.; Englander, S. W. *Nature* **1988**, *335*, 700-4.
- (17) Johnson, W. C., Jr. *Annual Review of Biophysics and Biophysical Chemistry* **1988**, *17*, 145-66.
- (18) Lattman, E. E. *Current Opinion in Structural Biology* **1994**, *4*, 87-92.
- (19) Elove, G. A.; Bhuyan, A. K.; Roder, H. *Biochemistry* **1994**, *33*, 6925-35.
- (20) Elove, G. A.; Chaffotte, A. F.; Roder, H.; Goldberg, M. E. *Biochemistry* **1992**, *31*, 6876-83.
- (21) Yeh, S.-R.; Takahashi, S.; Fan, B.; Rousseau, D. L. *Nature Structural Biology* **1997**, *4*, 51-56.
- (22) Takahashi, S.; Yeh, S. R.; Das, T. K.; Chan, C. K.; Gottfried, D. S.; Rousseau, D. L. *Nature structural biology* **1997**, *4*, 44-50.
- (23) Quinn, P. J.; Kagan, V. E.; Editors *Phospholipid Metabolism in Apoptosis: Subcellular Biochemistry, Volume 36. [In: Subcell. Biochem., 2002; 36]*, 2002.
- (24) McMillin, J. B.; Dowhan, W. *Biochimica et Biophysica Acta, Molecular and Cell Biology of Lipids* **2002**, *1585*, 97-107.
- (25) Jori, G.; Tamburro, A. M.; Azzi, A. *Photochemistry and photobiology* **1974**, *19*, 337-45.
- (26) Fedurco, M. *Coordination Chemistry Reviews* **2000**, *209*, 263-331.
- (27) Bertini, I.; Cavallaro, G.; Rosato, A. *Chemical Reviews (Washington, DC, United States)* **2006**, *106*, 90-115.
- (28) Dickerson, R. E.; Kopka, M. L.; Borders, C. L., Jr.; Varnum, J.; Weinzierl, J. E. *Journal of molecular biology* **1967**, *29*, 77-95.
- (29) Dickerson, R. E.; Kopka, M. L.; Weinzierl, J.; Varnum, J.; Eisenberg, D.; Margoliash, E. *Journal of biological chemistry* **1967**, *242*, 3015-8.

- (30) Bushnell, G. W.; Louie, G. V.; Brayer, G. D. *Journal of molecular biology* **1990**, *214*, 585-95.
- (31) Louie, G. V.; Brayer, G. D. *Journal of molecular biology* **1990**, *214*, 527-55.
- (32) Murgida, D. H.; Hildebrandt, P. *Journal of the American Chemical Society* **2001**, *123*, 4062-4068.
- (33) Khoshtariya, D. E.; Wei, J.; Liu, H.; Yue, H.; Waldeck, D. H. *Journal of the American Chemical Society* **2003**, *125*, 7704-7714.
- (34) Dolla, A.; Blanchard, L.; Guerlesquin, F.; Bruschi, M. *Biochimie* **1994**, *76*, 471-9.
- (35) Battistuzzi, G.; Borsari, M.; Sola, M.; Francia, F. *Biochemistry* **1997**, *36*, 16247-58.
- (36) Cruanes, M. T.; Rodgers, K. K.; Sligar, S. G. *Journal of the American Chemical Society* **1992**, *114*, 9660-1.
- (37) Bond, A. M. *Inorganica Chimica Acta* **1994**, *226*, 293-340.
- (38) Niki, K.; Hardy, W. R.; Hill, M. G.; Li, H.; Sprinkle, J. R.; Margoliash, E.; Fujita, K.; Tanimura, R.; Nakamura, N.; Ohno, H.; Richards, J. H.; Gray, H. B. *Journal of Physical Chemistry B* **2003**, *107*, 9947-9949.
- (39) Petrovic, J.; Clark, R. A.; Yue, H.; Waldeck, D. H.; Bowden, E. F. *Langmuir* **2005**, *21*, 6308-6316.
- (40) Wei, J.; Liu, H.; Khoshtariya Dimitri, E.; Yamamoto, H.; Dick, A.; Waldeck David, H. *Angewandte Chemie (International ed. in English)* **2002**, *41*, 4700-3.
- (41) Mathews, C. K.; van Holde, K. E.; Ahern, K. G. **2000**, 1186 pp.
- (42) Kerr, J. F.; Wyllie, A. H.; Currie, A. R. *British journal of cancer* **1972**, *26*, 239-57.
- (43) Hengartner, M. O. *Nature (London)* **2000**, *407*, 770-776.
- (44) Adams, J. M.; Cory, S. *Science (Washington, D. C.)* **1998**, *281*, 1322-1326.
- (45) Li, P.; Nijhawan, D.; Budihardjo, I.; Alnemri, E. S.; Wang, X. *Cell (Cambridge, Massachusetts)* **1997**, *91*, 479-489.
- (46) Zou, H.; Henzel, W. J.; Liu, X.; Lutschg, A.; Wang, X. *Cell (Cambridge, Massachusetts)* **1997**, *90*, 405-413.
- (47) Bard, A. J.; Faulkner, L. R. *Electrochemical Methods: Fundamentals and Applications*, 1980.

- (48) Kagan, V. E.; Tyurin, V. A.; Jiang, J.; Tyurina, Y. Y.; Ritov, V. B.; Amoscato, A. A.; Osipov, A. N.; Belikova, N. A.; Kapralov, A. A.; Kini, V.; Vlasova, I. I.; Zhao, Q.; Zou, M.; Di, P.; Svistunenko, D. A.; Kurnikov, I. V.; Borisenko, G. G. *Nature Chemical Biology* **2005**, *1*, 223-232.
- (49) Loetzbeier, T.; Schuhmann, W.; Schmidt, H.-L. *Journal of Electroanalytical Chemistry* **1995**, *395*, 339-43.
- (50) Huang, W.; Jia, J.; Zhang, Z.; Han, X.; Tang, J.; Wang, J.; Dong, S.; Wang, E. *Biosensors & Bioelectronics* **2003**, *18*, 1225-1230.
- (51) Hayashi, Y.; Yamazaki, I. *Journal of biological chemistry* **1979**, *254*, 9101-6.
- (52) Tatsuma, T.; Watanabe, T. *Analytical Chemistry* **1991**, *63*, 1580-5.
- (53) Van Rantwijk, F.; Sheldon, R. A. *Current Opinion in Biotechnology* **2000**, *11*, 554-564.
- (54) Erman, J. E.; Vitello, L. B. *Biochimica et Biophysica Acta, Protein Structure and Molecular Enzymology* **2002**, *1597*, 193-220.
- (55) Osman, A. M.; Koerts, J.; Boersma, M. G.; Boeren, S.; Veeger, C.; Rietjens, I. M. *European journal of biochemistry / FEBS* **1996**, *240*, 232-8.